Taylor & Francis
Taylor & Francis Group

Particulate Science and Technology

An International Journal

ISSN: (Print) (Online) Journal homepage: https://www.tandfonline.com/loi/upst20

Green synthesis of silver nanoparticles using flower extracts of *Aerva lanata* and their biomedical applications

Sashikiran Palithya, Susmila Aparna Gaddam, Venkata Subbaiah Kotakadi, Josthna Penchalaneni, Narasimha Golla, Suresh Babu Naidu Krishna & C. V. Naidu

To cite this article: Sashikiran Palithya, Susmila Aparna Gaddam, Venkata Subbaiah Kotakadi, Josthna Penchalaneni, Narasimha Golla, Suresh Babu Naidu Krishna & C. V. Naidu (2021): Green synthesis of silver nanoparticles using flower extracts of *Aerva lanata* and their biomedical applications, Particulate Science and Technology, DOI: 10.1080/02726351.2021.1919259

To link to this article: https://doi.org/10.1080/02726351.2021.1919259

Published online: 07 May 2021.

PARTICULATE SCIENCE AND TECHNOLOGY
https://doi.org/10.1080/02726351.2021.1919259

Taylor & Francis
Taylor & Francis Group

Green synthesis of silver nanoparticles using flower extracts of *Aerva lanata* and their biomedical applications

Sashikiran Palithya[a], Susmila Aparna Gaddam[b], Venkata Subbaiah Kotakadi[c], Josthna Penchalaneni[d], Narasimha Golla[b], Suresh Babu Naidu Krishna[e], and C. V. Naidu[a]

[a]Department of Biotechnology, Dravidian University, Kuppam, India; [b]Department of Virology, Sri Venkateswara University, Tirupati, India; [c]DST-PURSE Centre, Sri Venkateswara University, Tirupati, India; [d]Department of Biotechnology, Sri PadmavathiMahila University, Tirupati, India; [e]Department of Biomedical and Clinical Technology, Durban University of Technology–Steve Biko Campus, Durban, South Africa

ABSTRACT

In the present study, green synthesis of silver nanoparticles (AgNPs) was performed using flower extracts of *Aerva lanata* (Al) from Amaranthaceae family. The size, shape, and elemental composition of the silver nanoparticles (AgNPs) was studied using transmission electron microscopy (TEM), scanning electron microscopy (SEM), energy dispersive X-ray analysis (EDX), and UV-visible spectroscopy. The dynamic light scattering (DLS), of silver nanoparticles (AgNPs) exhibited mean size of 7.6 nm in the range of 5–15 nm, having a poly-dispersed indexed value of 0.419. Zeta potential contributing to the stability of silver nanoparticles was recorded as −18.7 mV. Transmission electron microscopy (TEM) and energy dispersive X-ray (EDX) analysis confirmed the presence of the synthesized AgNPs with an average size range 7 ± 3 nm. The biosynthesized silver nanoparticles displayed antibacterial activity against Gram-positive and Gram-negative bacteria. The 2,2′-Diphenyl-1-picrylhydrazyl (DPPH) radical scavenging assay revealed antioxidant potential of silver nanoparticles in the concentration of 100 µg/ml. The photocatalytic activity of silver nanoparticles was evaluated using decolourization of the dyes under the sunlight using UV-Vis. spectroscopy. The results suggest that biosynthesized silver nanoparticles from *A. lanata* (Al-AgNPs) flower extracts have broad spectrum antibacterial, antioxidant and catalytic activities may be useful in a variety of biomedical and industrial applications.

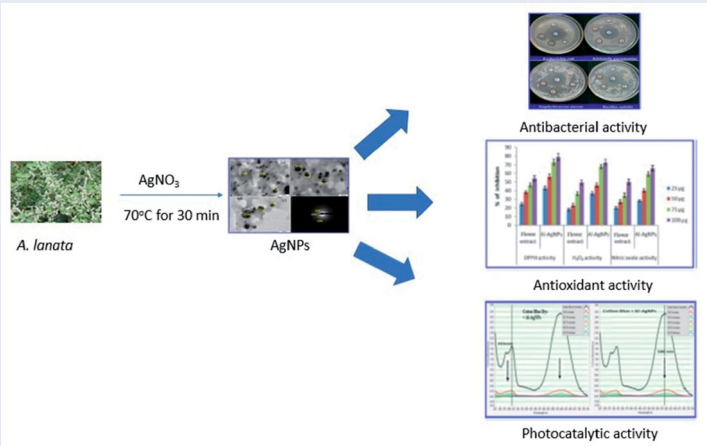

KEYWORDS

Aerva lanata; antibacterial activity; antioxidant activities; electron microscopy; spectral characterization; antibacterial resistance

1. Introduction

Nanotechnology has emerged as one of the most sought-after interdisciplinary research field in modern science and has shaped a vast range of research activities taken up in biological science and has provided the pavement for the development of advanced nanotechnological devices and tools. Nanomaterials that exist in the form of atoms and molecules at the level of billionth of a meter play a major role as the elementary building blocks of nanotechnology and have made an enormous impact on the mankind due to its simple, rapid, stable, economical, nontoxic and eco-friendly nature (Ijaz, Zafar, et al. 2020).

Metallic nanoparticles with unique size make them indispensable because, of larger surface area to volume ratio and find necessary applications in several areas such as catalysis, optics, electronics, display devices, pharmacy, medicine, material science, photonics, biological probes, drug delivery

CONTACT C. V. Naidu challgundlav@yahoo.co.in Department of Biotechnology, Dravidian University, Kuppam 517425 India.

systems, medical surgical implants, etc. (Ijaz, Aftab, et al. 2020; Naidu 2020; Saiganesh et al. 2021).

Recently, biogenesis approaches using plant extracts have gained much attention across worldwide because of low-cost production, faster synthesis rate, prevents agglomeration low toxicity and multipurpose morphological properties in comparison to microorganisms based green synthesis procedures. Many plants such as *Alfalfa, Amaranthus tricolor, Buddleja globose, Coriandrum sativum, Cassia alata, Datura metel, Geranium leaf, Lemon grass* have shown the potentiality of reducing nature for the formation of AgNPs with differences with respect to their size, shape, stability and synthesis conditions (Gaddam et al. 2014; Fatimah and Aftrid 2019; Ijaz, Zafar, et al. 2020). The AgNPs in the colloidal state have widely been used to research the catalytic action in the model reaction is electron exchange reaction between hexacyanoferrate (III) to hexacyanoferrate(II) (Emam, Zahran, and Ahmed 2017). According to the studies of (Seku et al. 2018) microwave assisted synthesis of AgNPs from potential catalytic activity was examined utilizing an electron exchange reaction between hexacyanoferrate (III) and $NaBH_4$. The Synthesized AgNPs using carboxymethylation gum kondagogu enhances the stability of nanoparticles, as well as the *Andrographis serpyllifolia* synthesized AgNPs showed good catalytic and biological activities. Similarly, the catalytic activity of phyto mediated AgNPs from *Plectranthus amboinicus* leaf extracts showed in terms of the reduction of 4-nitrophenol (Reddy et al. 2017).

Aerva lanata (local name: Konda pindi) is a rare medicinal plant used in traditional medicine from Amaranthaceae family. *Aerva lanata* is particularly known as mountain knot grass and it grows everywhere as a prostrate, perennial shrub and mostly found in the mountain plains of different parts of India (Goyal et al. 2011). Pharmacognostic studies and phytochemical screenings of *A. lanata* have shown the presence of various classes of phytochemicals such as alkaloids, aromatics, amides, alcohols, alkanes, carboxylic acids, steroids, flavonoids, tannins, amino acids, proteins, carbohydrates, glycosides, saponins, terpenoids and biological activities. The flowers of *A. lanata* perform several biological activities such as anti-urolithiatic (Silvia et al. 2014), antidiabetic, anti-inflammatory (Payal et al. 2015), analgesic (Athira and Nair 2017), diuretic (Abdulmutalib and Manjur 2017), antinociceptive (Nagaratna et al. 2015), antiasthamatic (Vidhya and Udayakumar 2015), antibacterial (Kirubha and Alagumuthu 2015) and antioxidant properties (Paramasivam et al. 2012).

Considering the above, the present study aims to biosynthesize eco-friendly AgNPs using the flower extracts of *A. lanata*. Silver Nanoparticles synthesized from flower extracts were characterized in terms of composition/quality and functional groups responsible for capping and bio-reduction of AgNPs confirmed by UV-Vis spectroscopy, Fourier transform infrared spectroscopy (FTIR), Dynamic light scattering (DLS), Zeta potential, Energy dispersive X-ray (EDX) and Transmission electron microscopy (TEM) and biological activities like antibacterial, antioxidant and catalytic properties were studied.

2. Materials And methods

2.1. Green synthesis of silver nanoparticles

The flowers of *A. lanata* were identified and collected from the herbs and shrubs growing in and around the farmland region of Sri Venkateswara Agricultural University and Sri Venkateswara University, Tirupati, Chittoor district of Andhra Pradesh state, India during the months of October and November (Figure 1). The flowers of *A. lanata* were collected, shade dried for a week at room temperature and then made into fine powder with the help of electric blender. The plant flower extracts of *A. lanata* were prepared, by adding 5 g of finely powder leaves in a 500 ml Erlenmeyer flask with 250 ml of Milli Q ultra-pure distilled water and the mixture was heated at 70 °C for 30 min and then filtered through sterile muslin cloth followed by Whatman No.1 filter paper. This filtrate solution was used as a source of extract for preparation of silver nanoparticles and was utilized in subsequent procedures. To the 5 ml diluted filtrate, 10 ml of 0.002(M) $AgNO_3$ was added and the sample was left at room temperature, until the color of solution changed from pale light green color to light brown color and subsequently dark brown. The solution containing biosynthesized silver nanoparticles (Al-AgNPs) were confirmed by the dark brown color change (Hussain et al. 2016). So, in the present study the biosynthesis of silver nanoparticles (Al-AgNPs) using the plant flower extract of *A lanata* were prepared without using any other toxic chemicals by "Green synthesis" method.

2.2. UV-Vis spectrophotometry

Noble metal nanoparticles absorb strongly in the visible region due to surface plasmon resonance. Hence, UV-visible absorption spectroscopy acts as a primary characterization tool for the study of metal nanoparticle formation and proved to be a very useful technique for the analysis of nanoparticles. The bio-reduction of $Ag+$ ions by using the plant flower extracts of *A. lanata* were monitored from time to time by sampling of the 1 µl aliquots and the UV-Vis absorbance spectra was monitored and recorded on the Nanodrop- 8000 UV-Vis spectrophotometer in 220–700 nm wavelength range. (Sri Venkateswara University, Tirupati).

2.3. Fourier transform infrared (FTIR)

The FTIR spectral analysis of the biosynthesized Al-AgNPs provides the information regarding the formation of crystalline nanoparticles and the presence of functional groups in the sample. This profile is in the form of an absorption spectrum which shows the peaks representing components in higher concentration that depicts the presence of different types of bonds, and different functional groups (e.g., alkanes, ketones, amines, halides), absorb infrared radiation of different wavelengths. The identification of possible biomolecules responsible for the reduction and stabilization of the biosynthesized Al-AgNPs were monitored and recorded using the

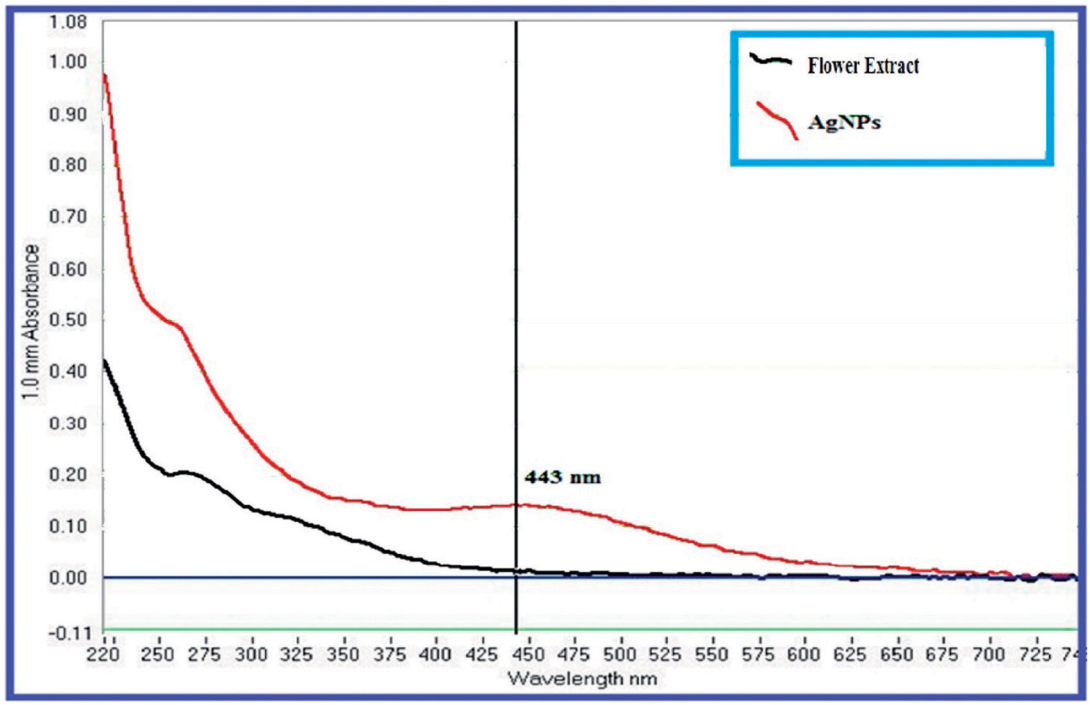

Figure 1. UV-Visible spectra of *Aerva lanata* flower extract and biosynthesized Al-AgNPs.

instrument Brucker Tensor 27, Thermo Scientifics, USA. (Sri Venkateswara University, Tirupati).

2.4. Dynamic light scattering (DLS) particle size analysis and zeta potential

The particle size of the biosynthesized Al-AgNPs was detected by the DLS intensity and laser diffraction method using the biosynthesized colloidal solution, in which the Al-AgNPs are poly-dispersed in mixture solution. The DLS analysis was used for measurement of average hydrodynamic diameters and poly dispersity indexes (PDI) of the Al-AgNPs. The Zeta potential analysis of the biosynthesized Al-AgNPs was also carried out for studying the negative potential value that provides the reduction and stability of biosynthesized Al-AgNPs due to electrostatic repulsive force that avoids the formation of agglomeration of Al-AgNPs. The DLS particle size analysis and Zeta potential analysis of the biosynthesized Al-AgNPs were carried out by means of laser diffractometry using Horiba Nanopartica SZ-100 instrument. (Sri Venkateswara University, Tirupati).

2.5. X-ray diffractometry (XRD)

The crystalline structure of the biosynthesized Al-AgNPs was studied from their XRD patterns. The XRD pattern measurements of the bio-reduced silver colloidal solution (Al-AgNPs) was applied as drop coated onto a glass substrate were recorded in a wide range of Bragg angle 2θ at a scanning rate of 2° min^{-1}, carried out using the instrument ULTIMA IV-X-ray powder diffractometer (RIGAKU LTD, Tokyo, Japan) by means of Cu radiation source, Madras University, Chennai, India.

2.6. Energy dispersive absorption X-ray spectroscopy (EDAX)

Energy dispersive analysis of X-rays (EDAX) is a chemical microanalysis technique that utilizes the X-rays that are emitted from the sample during bombardment by the electron beam to characterize the elemental composition of the analyzed volume of silver nanoparticle sample (Al-AgNPs). The EDX analysis was performed by using the instrument Oxford Inca Penta FeTX3 EDS instrument was attached to Carl Zeiss EVO MA 15 scanning electron microscope (200 kV) with a line resolution 2.32 A^{o}. (Sri Venkateswara University, Tirupati).

2.7. Transmission electron microscopy (TEM) studies

Transmission electron microscopy (TEM) analysis was conducted to study the size and shape of surface morphology and topology of the biosynthesized Al-AgNPs. TEM attached with Energy dispersive analysis of X-rays (EDS) and Selected area electron diffraction (SAED) analyses were used. The biogenic Al-AgNPs were washed and diluted by water to attain the absorbance range 0.5. Further, one drop of diluted Al-AgNPs sample was placed on Cu grid with Uranium Cu on Holey carbon disk and was allowed to dry in vacuum. Then, the nanoparticles were visualized using 200 kV FEI-Tecnai G2 20 S-TWIN High resolution TEM (Vellore Institute of Technology, Vellore, India).

2.8. Antibacterial activity of the biosynthesized AL-AgNPs by disc diffusion method

The antibacterial activity of the biosynthesized silver nanoparticles (Al-AgNPs) obtained from the plant flower extracts

of *A. lanata* were effectively tested by standard Disk diffusion method (Bauer et al. 1996) against Gram positive *Staphylococcus aureus, Bacillus subtilis* and Gram negative *Klebsiella pneumonia, Escherichia coli.* acquired from DST-PURSE Center, Sri Venkateswara University, Tirupati. The sterile disk of WhatmanNo.1 filter paper of about 5 mm diameter was prepared and was soaked in Al-AgNPs solution (10 µl, 20 µl and 30 µl) and allowed to dry before being placed on the agar plate, along with the disks prepared from plant extract, $AgNO_3$ and the standard disk of Amoxyclav (Hi-media SD063). The cultures were incubated at 37° C for 24 hours in an incubator. Later, the plates were observed and measured for zones of inhibition (ZOI) against each type of microorganism.

2.9. Antioxidant activity of the biosynthesized Al-AgNPs

The antioxidant activity of the biosynthesized Al-AgNPs were evaluated *in-vitro* by three methods viz. 2,2′-Diphenyl-1-picrylhydrazyl (DPPH) radical scavenging activity, Nitric oxide (NO) radical scavenging activity and Hydrogen peroxide (H_2O_2) radical scavenging activity, using Ascorbic acid as a standard control.

2.9.1. DPPH radical scavenging activity

The in-vitro antioxidant activity of Al-AgNPs was measured and recorded by 2,2′-Diphenyl-1-picrylhydrazyl (DPPH) radical scavenging assay (Gupta et al. 2014). Briefly, 4 mg of DPPH was dissolved in 100 ml of methanol and stored at 20° C. From the stock solution, 2 ml of the solution was added to 1 ml of methanol solution containing test samples of *A. lanata* flower extract and Al-AgNPs at various concentrations of 25, 50, 75, and 100 µg/ml. After a 30 min incubation period at room temperature, the absorbance was measured at 517 nm. The percentage of inhibition of free radical scavenging activity was calculated using Equation (1) as given below,

$$\text{Radical Scavenging Activity} = \frac{(\text{Ac} - \text{As})}{(\text{Ac})} \times 100 \quad (1)$$

Where "A_C" stands for the absorbance of the control reaction and "A_S" stands for the absorbance of the test compound (i.e., the plant extracts and the Al-AgNPs), the tests were carried in triplicate.

2.9.2. Nitric oxide scavenging activity

Nitric oxide scavenging activity was measured by method as described by Kumar, Paul, and Sharma (2011) with slight modifications. Nitric oxide radicals (NO) were generated from sodium nitroprusside. 1 ml of sodium nitroprusside (10 mM) and 1.5 ml of phosphate buffer saline (0.2 M, pH 7.4) were added to different concentrations of 25, 50, 75 and 100 µg/ml of the test compounds (plant extracts and Al-AgNPs) and incubated for 150 min at 25 °C; 1 ml of the reaction mixture was treated with 1 ml of Griess reagent (1% sulphanilamide), 2% H_3PO_4 and 0.1% naphthyl ethylene diamine dihydrochloride. The absorbance of the compounds was measured at 546 nm. The percentage of nitric oxide scavenging activity was calculated using Equation (1) as mentioned above.

2.9.3. Hydrogen peroxide scavenging activity

Hydrogen peroxide (H_2O_2) scavenging ability of the test compounds (plant extracts and Al-AgNPs) was determined according to the literature method (Revathi et al. 2014). A solution of H_2O_2 (40 mM) was prepared in phosphate buffer (pH 7.4). 25, 50, 75 and 100 µg/ml concentrations of the test compounds (i.e., plant extracts and Al-AgNPs) in 3.4 ml phosphate buffer were added to H_2O_2 solution (0.6 ml, 40 mM). The absorbance value of the reaction mixture was recorded at 230 nm. The percentage of H_2O_2 scavenging activity was calculated using Equation (1) as mentioned above.

2.10. Catalytic activity of the biosynthesized Al-AgNPs

2.10.1. Photocatalytic activity degradation of dyes

The photocatalytic activity of the biosynthesized Al-AgNPs was evaluated by using the natural dyes Cotton blue (10 mg l^{-1}) and Congo red (10 mg l^{-1}) aqueous solutions were prepared and set for conduct. Further, these solutions were exposed to the outdoors under the sunlight as the energy source for the conduction of the photocatalytic reactions. The cotton blue (CB) and congo red (CR) dye solutions along with the suspension of the biosynthesized Al-AgNPs were prepared and setup for the conduction of the experiment, for bringing the biosynthesized Al-AgNPs to constant equilibrium, the mixture solutions were exposed to the stirring for 30 min. in the dark. Afterwards, this mixture solution was exposed to the sunlight and kept undisturbed for 5–6 h. Then the mixture solution was centrifuged for confirming the phyto-detoxification of the dye and the absorbance OD values were noted at regular intervals until the solution showed color change and became completely colorless. The above experiment was performed at ambient temperature and at pH of 6.5. The absorbance OD values were recorded on the UV-Vis spectrophotometer.

2.10.2. Catalytic activity in reduction of 4-Nitrophenol:

The reduction of toxic 4-Nitrophenol (4-NP) to nontoxic 4-Aminophenol (4-AP) was performed to know the potentiality of the biosynthesized Al-AgNPs for their catalytic activity (Wunder et al. 2010). In this procedure, 2 ml (0.08 mM) 4-NP was added to a 3 ml quartz cuvette (1 cm path length) and 0.5 ml (0.08 mM) freshly prepared $NaBH_4$was added to this. Further, 0.3 ml of the biosynthesized Al-AgNPs was added, all the reactions are known to follow the pseudo-first-order decay kinetics. The reduction reaction of 4-NP to 4-AP was monitored by the UV-Vis spectrophotometer, which shows the UV-Vis spectra of the reduction of 4-NP by $NaBH_4$ in the presence of Al-AgNPs as a catalyst as well. The UV-Vis absorption spectra were recorded for every 5 min time interval in the wavelength range of 200–800 nm.

3. Results and discussion

3.1. Biosynthesis of silver nanoparticles from flower extracts of Aerva lanata

The biosynthesis of silver nanoparticles (Al-AgNPs) using $AgNO_3$ solution through a simple green method using the plant flower extracts of *A. lanata* as reducing and as capping agent (Figure 1). The solution containing the colorless flower extract of *A. lanata* was changed into dark brown color within few minutes after the addition of 0.002 M $AgNO_3$ solution. Therefore, confirmed the reduction of $AgNO_3$ and formation of silver nanoparticles (Al-AgNPs) of *A. lanata*, without the use of any toxic chemicals. Since the reduction time was within 5–10 min, similar reports (Seku et al. 2018) and (Vaishnavi et al. 2020) where AgNPs from plant extracts of *Ziziphus jujuba* Mill (ZJM) fruit and *Pterocarpus santalinus* respectively reduced the filtrate from green to brown color. Hence, it is concluded that this is an eco-friendly method known as "green method or green synthesis."

3.2. Ultraviolet–visible spectroscopy

The UV-Vis spectra of the sample solution (Al-AgNPs) showed a sharp and strong absorbance peak at 443 nm (Figure 1) which is a characteristic surface plasmon resonance (SPR) peak of silver nanoparticles and hence confirmed the formation of AgNPs and their synthesis. This also indicates that the biosynthesized silver nanoparticles (Al-AgNPs) were small and round. The several bio-compounds and functional groups present in the *A. lanata* plant flower extract could be responsible for bio reduction and capping of Al-AgNPs synthesized. It was evident from the earlier studies that, the particles under the SPR range between 420 and 450 nm were attributed to AgNPs comprising of varying sizes between 2 and 100 nm (Iqbal et al. 2020).

3.3. Fourier transform infrared (FTIR)

The FTIR spectral analysis of Al-AgNPs (Figure 2(a)) showed the sharp peaks at, 3841 cm^{-1}, 3735 cm^{-1}, 3613 cm^{-1}, and 3200cm^{-1} that corresponds to N–H, O–H, O–H, and N–H stretching vibrations of secondary amines, alcohols, and amides group (Netala et al. 2016). The peaks observed at 2434 cm^{-1}, 2352 $cm^{-1,}$ and 1640 cm^{-1}corresponding to C≡C, C≡C, and C = C stretching vibrations of carbonyl and aromatic groups. The peaks observed at 1530 cm^{-1}, 1395 cm^{-1}corresponding to CH– and C–O stretching vibrations of amide linkage of proteins. The peaks observed at 1242 cm^{-1} and 1032 cm^{-1} corresponding to C–OH and C–C stretching vibrations of carboxylic acids (Netala et al. 2018). The peaks observed at 668 cm^{-1} and 534 cm^{-1} corresponding to C–Cl and C–Br stretching vibrations of Halides groups. FTIR analysis clearly reveals that the participation of phytochemicals like carboxylic acids, proteins and polyphenols present in the plant flower extract were mainly responsible for the bioreduction of silver ions (Ag^+) into nano silver particles (Ag^0). And also other bio compounds such as the flavonoids, phenols, alkaloids, alcohols, saponins, aromatics, etc. also played role in the stabilization of Al-AgNPs by acting as capping agents and preventing the agglomeration of the Al-AgNPs.

3.4. Dynamic light scattering (DLS) particle size and zeta potential

The particle size of the biosynthesized Al-AgNPs was detected by dynamic light intensity and laser diffraction method. The DLS data showed about the size distribution of the biosynthesized Al-AgNPs by measuring their effects in light scattering due to the Brownian motion of the AgNPs in liquid solution. The biosynthesized Al-AgNPs were in the range of 5 nm to 15 nm with an average size of 7.6 nm (Figure 2(b)), with a poly dispersed index value of 0.419 was observed. The DLS analysis data reveals that results are in correlation with UV-Vis analysis i.e., if the SPR region of AgNPs were in between 400 abd 470 nm, the nanoparticles are said to be small and spherical in size (Gaddam et al. 2014; Kotakadi et al. 2015). The Zeta potential analysis is one of the important characterization parameters that shows the presence of charge on the AgNPs in a particular medium. In general, the nanoparticles (NPs) exhibit charge on their surface, due to which a repulsive force is created among the NPs that leads to the non-formation of agglomeration of the NPs, leading to a long-term stability of NPs. The Zeta potential analysis data of the biosynthesized Al-AgNPs was −18.7 mV (Figure 2(c)), indicating the presence of negative charge on the surface of Al-AgNPs, avoiding the formation of agglomeration in the medium and a moderate long-term stability was formed. The earlier reports revealed that the NPs having the charge in the range of +30 mV to −30 mV were very much stable (Suresh et al. 2011; Kotakadi et al. 2016) and in the range of +15 mV to −25 mV were moderately stable (Kotakadi et al. 2015).

3.5. Energy-dispersive X-ray spectroscopy (EDX)

The EDX analysis data of the biosynthesized Al-AgNPs showed a very strong signal in the silver region, which confirmed the formation of AgNPs that might have originated due to the presence of the biomolecules bound to the surface of Al-AgNPs. The EDX analysis revealed the presence of elemental silver with 63.44% of silver (Figure 2(d)), 21.37% of aluminum, 8.03% of oxygen, 6.25% of chlorine, 0.38% magnesium, 0.32% of potassium, 0.19% of sodium, 0.03% of calcium, 0.01% of iron and −0.14% of manganese elements were present overall, which might have originated from the biomolecules that were bound to the surface of Al-AgNPs, confirmed the complete reduction of silver ions (Dauthal and Mukhopadhyay 2013). In general, the metallic AgNPs showed an absorption peak approximately at 3 KeV due to the surface plasmon resonance (SPR)(Ajitha, Reddy, and Reddy 2015).

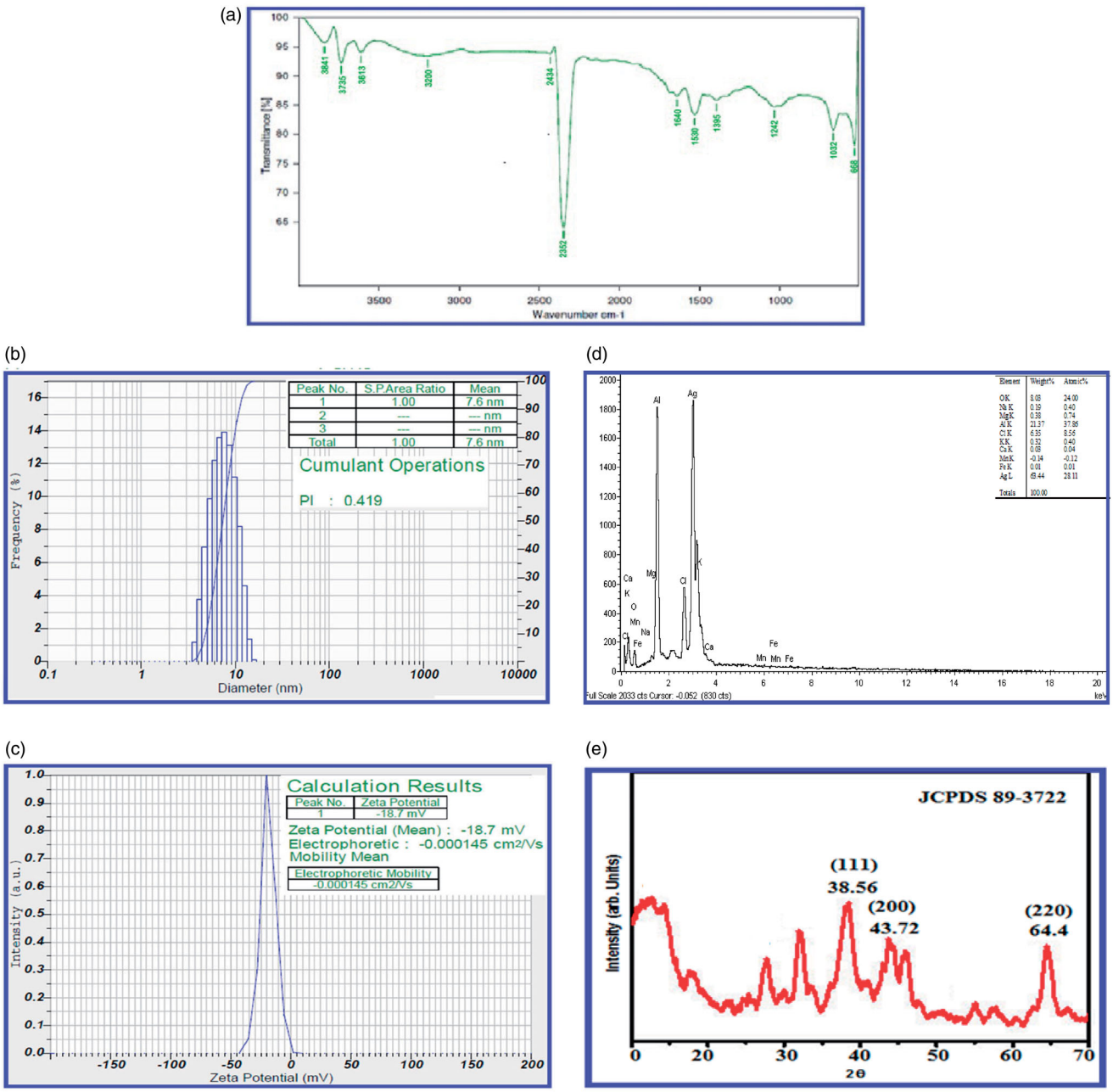

Figure 2. (a) FTIR spectrum of silver nanoparticles synthesized from *Aerva lanata* flower extracts. (b) DLS Particle size distribution curve of silver nanoparticles derived from *A. lanata* flower extracts. (c) Zeta potential of silver nanoparticles. (d) EDX spectrum of silver nanoparticles synthesized from flower extracts *A. lanata*. (e) XRD spectrum of silver nanoparticles.

3.6. X-ray diffraction analysis (XRD)

X-ray diffraction (XRD) analysis is an advanced characterization spectroscopic technique that was used to evaluate the crystalline nature of biosynthesized Al-AgNPs. The XRD pattern showed three distinctive diffraction peaks (Figure 2(e)) corresponding to their respective planes at 38.56° (111), 43.72° (200), and 64.4° (220). The planes were indexed according to the facets of face centered cubic (FCC) crystal structure of silver (JCPDS card No. 89-3722). The XRD patterns were found to be like that of the earlier reports (Ghosh et al. 2012; Khatami et al. 2018).

3.7. Transmission electron microscopy (TEM)

TEM analysis was performed to determine the morphology and size of the biosynthesized Al-AgNPs. The TEM image analysis at various magnifications showed that the biosynthesized Al-AgNPs were poly-dispersed in nature, spherical in shape, and the size was in the range of 2–10 nm with an average size of 7 ± 3 nm (Figure 3(a–c)). The SAED pattern (Figure 3(d)) showed Debye-Scherrer rings corresponding to (111), (200), and (220) planes of the FCC crystal structure. The SAED pattern was also confirmed and like that of the XRD spectra analysis of Al-AgNPs. The results are in agreement with earlier reports of the biosynthesized

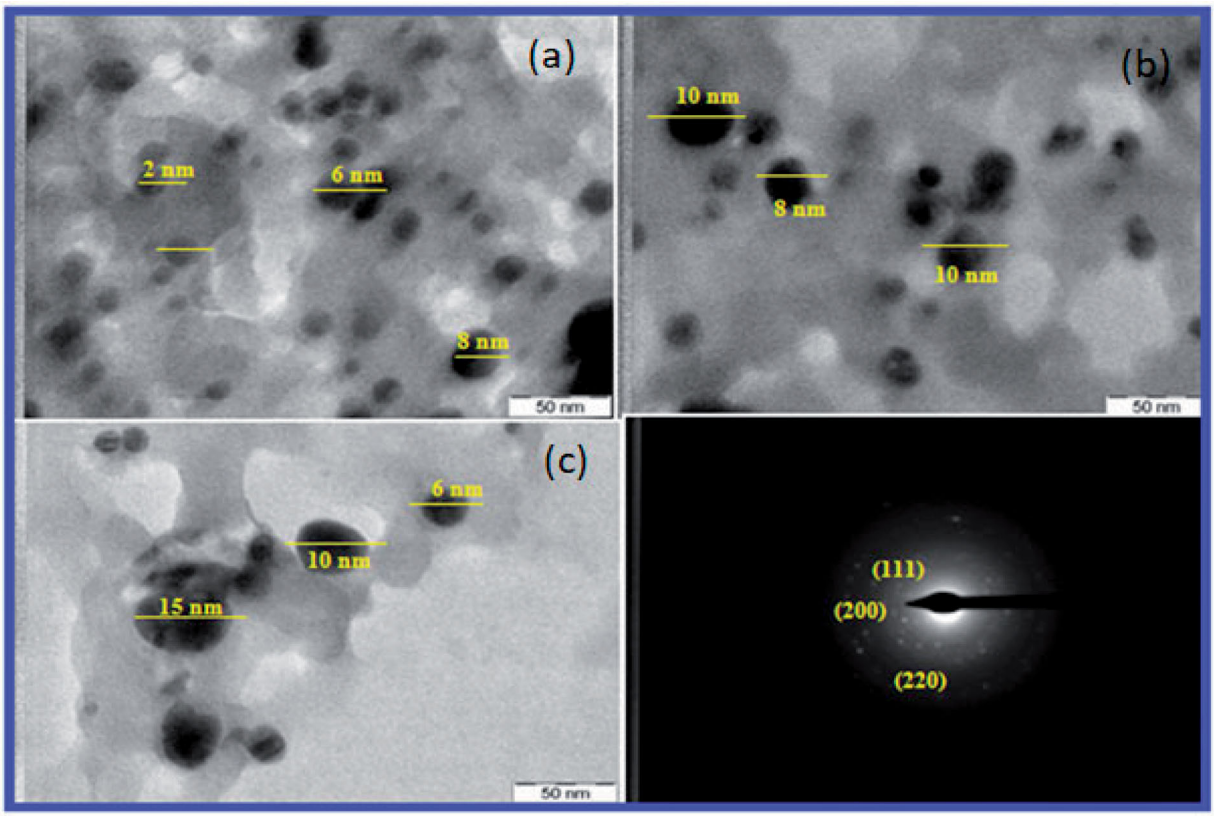

Figure 3. TEM images of the biosynthesized Al-AgNPs at magnification of (a) ×200 K, (b,c) ×360 K, (d) SAED pattern showed three diffraction rings.

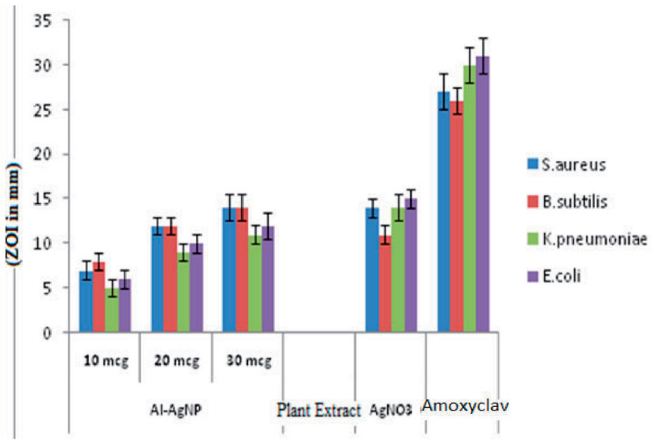

Figure 4. Antibacterial activity of silver nanoparticles synthesized using *A. lanata* flower extracts.

AgNPs obtained from different plant mediated sources (Litvin and Minaev 2013; Rauwel et al. 2015). The AgNPs from *Ziziphus nummularia* plant leaf extracts showed the size in spherical and uniform and size from 33 nm to 89 nm (Golla 2018).

3.8. Biomedical applications of the biosynthesized Al-AgNPs—antibacterial activity

In the present study to reveal the biomedical importance of the biosynthesized Al-AgNPs from flower extracts of *A. lanata* were used to study the antibacterial activity against four bacterial species *viz.* Gram-positive—*Staphylococcus aureus, Bacillus subtilis,* and Gram-negative—*Escherichia coli* and *Klebsiella pneumonia* by following the Kirby–Bauer Disk diffusion method. The biosynthesized Al-AgNPs exhibited very good antibacterial activity against *Bacillus subtilis* with the zone of inhibition (ZOI) of 08 mm, 12 mm, 14 mm at 10 mcg, 20 mcg, 30 mcg concentrations and against *E. coli* with the zone of inhibition of 06 mm, 10 mm,12 mm at 10 mcg, 20 mcg, 30 mcg concentrations, respectively. Hence, the biosynthesized Al-AgNPs showed very good antibacterial activity against both Gram-positive and Gram-negative bacteria (Figure 4) and moderate activity with that of control i.e., Amoxyclav antibiotic (Hi-media SD063) at the concentration 30 mcg (Figure 4; Table 1). The results were similar to that of the earlier reports (Netala et al. 2018; Afsheen et al. 2020).

3.9. Antioxidant activity

The antioxidant activity of the biosynthesized Al-AgNPs and the plant flower extracts of *A. lanata* showed very good results by all the three different methods used i.e., DPPH antioxidant activity, Hydrogen peroxide antioxidant activity and the Nitric oxide antioxidant activity.

3.9.1. DPPH scavenging activity

The antioxidant activity of the biosynthesized Al-AgNPs was performed by the DPPH scavenging activity method. The

DPPH free radical activity depends on the reduction of DPPH to DPPH-H, a hydrogen donating antioxidant. The in-vitro antioxidant activity results (Figure 5; Table 2) showed that the antioxidant free radical scavenging activity increased with the increase in the concentration (25 µg/ml, 50 µg/ml, 75 µg/ml, and 100 µg/ml) of the test samples i.e., the biosynthesized Al-AgNPs and the plant flower extract. The free radical scavenging activity results of the biosynthesized Al-AgNPs at 100 µg/ml was 78.96 ± 3.96 and that of the plant flower extract was 54.14 ± 2.97. Therefore, it was concluded that the biosynthesized Al-AgNPs showed very good free radical scavenging activity when compared to the plant flower extract. The biosynthesized Al-AgNPs by the plant flower extract consists of several secondary metabolites that includes flavonoids, tannins, carotenoids, lycopenes, carbohydrates, triterpenoids, glycosides, phenolic compounds, steroids, canthin-6-one and β-caroline alkaloids and other classes of phytoconstituents, etc. (Khan and Sultana 2006). The secondary metabolites can easily donate the hydrogen atoms, thus increasing the free radical scavenging activity of the biosynthesized Al-AgNPs, which in turn are actively involved in the stabilization of Al-AgNPs. This was also confirmed by the FTIR analysis data earlier. The results were similar to that of the earlier reports on the biosynthesized AgNPs from the plant extracts (Ramamurthy et al. 2013; Tamilarasi and Meena 2020; Turunc, Kahraman, and Binzet 2021).

Table 1. Antibacterial activity of biosynthesised silver nanoparticles against bacteria.

	Al-AgNPs		
Microorganism	10 mcg	20 mcg	30 mcg
S. aureus	7 ± 1	12 ± 1	14 ± 1.5
B. subtilis	8 ± 1	12 ± 1	14 ± 1.5
K. pneumoniae	5 ± 1	9 ± 1	11 ± 1
E. coli	6 ± 1	10 ± 1	12 ± 1.5
Control (Amoxyclav)	15 ± 1.5	15 ± 1.5	15 ± 1.5

The table indicates the Mean values of triplicates with standard deviation.

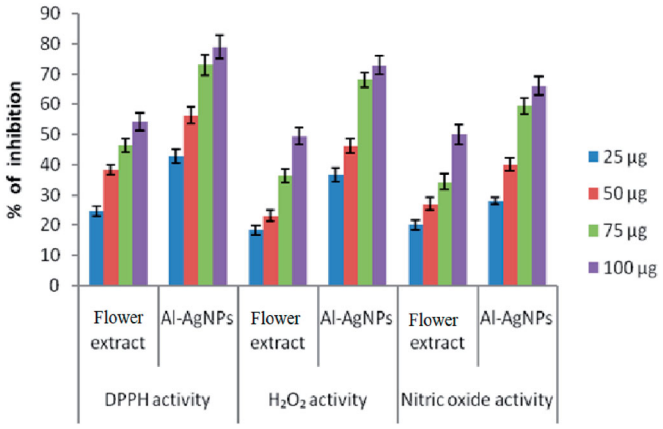

Figure 5. Antioxidant activity by DPPH method, hydrogen peroxide method and nitric oxide method.

3.9.2. Hydrogen peroxide scavenging activity

The accumulation of hydrogen peroxide in the living cells leads to an increase in the reactive oxygen species (ROS) such as the hydroxyl and peroxides that cause severe damage to the cell membrane. The hydrogen peroxide free radical scavenging activity was carried out on the test samples i.e., the biosynthesized Al-AgNPs and the plant flower extract of *A. lanata*. The H_2O_2 scavenging activity results of the biosynthesized Al-AgNPs at 100 µg/ml concentration was 72.86 ± 3.06 and plant flower extract of *A. lanata* was 49.47 ± 2.73 (Figure 5; Table 2). When compared to the results of the DPPH scavenging activity, the H_2O_2 scavenging activity result was lower. The H_2O_2 scavenging activity results are in agreement to that of the earlier reports (He et al. 2012; Mata, Nakkala, and Rani Sadras 2015; Al-Shmgani et al. 2017).

3.9.3. Nitric oxide scavenging activity

The nitric oxide (NO) is one of the important bioregulatory molecules which plays a vital role in the few biological systems such as the cardiovascular system, nervous system, immune system (Rees, Palmer, and Moncada 1989). Since the NO free radicals are very unstable in nature, this could be due to the formation of free radicals may be due to the interaction of AgNPs and NO under anhydrous condition at room temperature (Rodríguez-Gattorno et al. 2002). The nitric oxide free radical scavenging activity was carried out on the test samples i.e., the biosynthesized Al-AgNPs and the plant flower extract of *A. lanata*. The NO scavenging activity results of the biosynthesized Al-AgNPs at 100 µg/ml concentration was 66.08 ± 3.12 and plant flower extract of *A. lanata* was 50.08 ± 3.34 (Figure 5; Table 2). When compared to the results of the DPPH scavenging activity and the H_2O_2 scavenging activity, the NO scavenging activity result was lower than both. The NO scavenging activity results were similar to that of the earlier reports (Francis et al. 2018). The NO scavenging activity results showed that the biosynthesized Al-AgNPs could be used in the future antioxidant formulations.

3.10. Catalytic activity

The catalytic activity of the biosynthesized Al-AgNPs obtained from the flower extracts of *A. lanata* were used to

Table 2. Antioxidant activity of Al-AgNPs by DPPH, hydrogen peroxide, and nitric oxide methods.

	DPPH activity		Hydrogen peroxide activity		Nitric oxide activity	
Concentration	Flower extract	Al-AgNPs	Flower extract	Al-AgNPs	Flower extract	Al-AgNPs
25 µg	24.64 ± 1.65	42.84 ± 2.43	18.42 ± 1.45	36.72 ± 2.24	20.06 ± 1.51	27.98 ± 1.12
50 µg	38.34 ± 1.72	56.34 ± 2.84	23.18 ± 1.65	46.24 ± 2.45	27.06 ± 2.01	40.02 ± 2.1
75 µg	46.4 ± 2.35	72.98 ± 3.49	36.46 ± 2.32	68.1 ± 2.34	34.24 ± 2.6	59.46 ± 2.56
100 µg	54.14 ± 2.97	78.96 ± 3.96	49.47 ± 2.73	72.86 ± 3.06	50.08 ± 3.34	66.08 ± 3.12

The table indicates the mean values of the three readings with standard deviation.

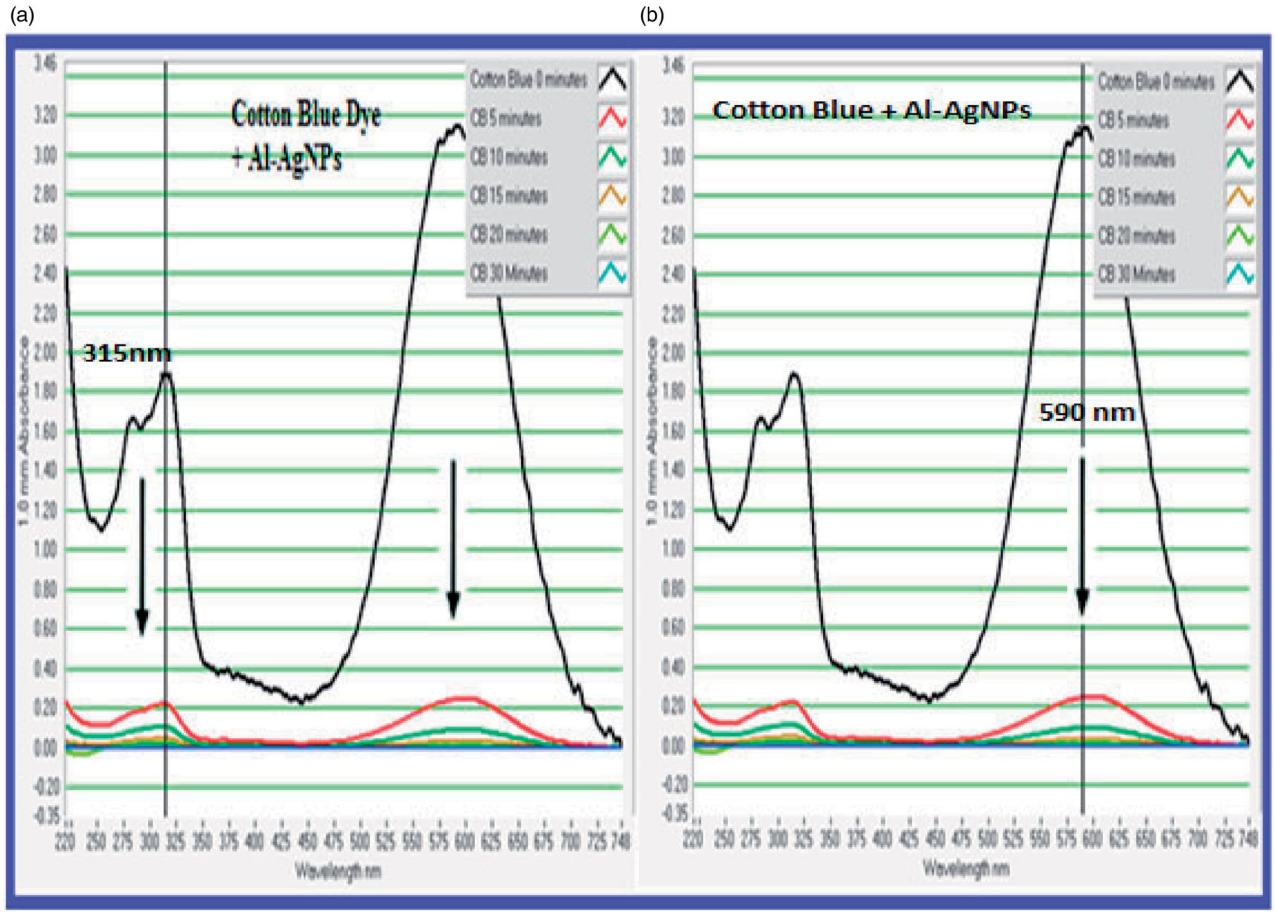

Figure 6. (a) UV-Vis spectra of cotton blue dye degradation at different time intervals. (b) Cotton blue dye degradation—UV-Vis spectra absorbance at different time intervals.

Table 3. UV-Vis spectra of cotton blue dye degradation at different time intervals by silver nanoparticles.

S. no.	Time interval (min)	315 nm	590 nm
1	0	1.894	3.092
2	5	0.217	0.244
3	10	0.100	0.087
4	15	0.044	0.029
5	20	0.024	0.011
6	30	0.009	0.006

study the photocatalytic degradation of the dyes industrial dyes and the reduction of toxic chemical 4-nitrophenol processes.

3.10.1. Photocatalytic degradation of dyes

The photocatalytic activity of the biosynthesized Al-AgNPs were determined by using the detoxification of the dyes Cotton blue (CB) and Congo red (CR) under the sunlight for a specific time. Firstly, the catalytic degradation of the dyes CB and CR in the presence of the biosynthesized Al-AgNPs were observed by change in color. The color intensities of the dyes CB changed from dark blue to light blue and for the dye CR changed from dark red to light red color, and therefore confirmed an effective catalytic dye degradation activity of the biosynthesized Al-AgNPs in the presence of sunlight. Further, the absorbance band values of the dye solutions (CB and CR) were taken, and the results were confirmed. Cotton blue dye is an aromatic cationic dye, used extensively by the textile industries for various purposes. The contaminated wastewater released by the industrial wastes lead to the several types of toxic effects such as skin irritation problems, gastrointestinal tract problems, eye irritation problems, etc. (Oliveira et al. 2008). The photocatalytic degradation result of CB was determined by the decreasing intensity of the absorbance band values corresponding to the time under the exposure of sunlight. The decrease in the peak intensity could be due to the SPR property of the biosynthesized Al-AgNPs. A similar type of work was earlier carried out with the maximum degradation of CB that was attained after a time interval of 77 h (Vanaja et al. 2014). In the present study, the CB solution was exposed for a time interval of 30 min. which exhibited significant decrease in the peak intensity (Figure 6; Table 3).

Congo red (CR), is a secondary diazo anionic dye, is majorly used in the dye industries. CR dye is a toxic carcinogenic metabolite, benzidine of CR leads to bladder cancer in humans. The effluents with the CR dye are highly colored possess high chemical oxygen demand in addition to high amounts of dissolved solids (Maiti, Purakayastha, and Ghosh 2007). The photocatalytic degradation of CR dye was monitored on Nanodrop 8000 UV-Vis spectrophotometer, which showed a gradual decrease of the peak intensity which was due to the presence of Al-AgNPs, confirmed the photocatalytic degradation of the CR dye. The degradation

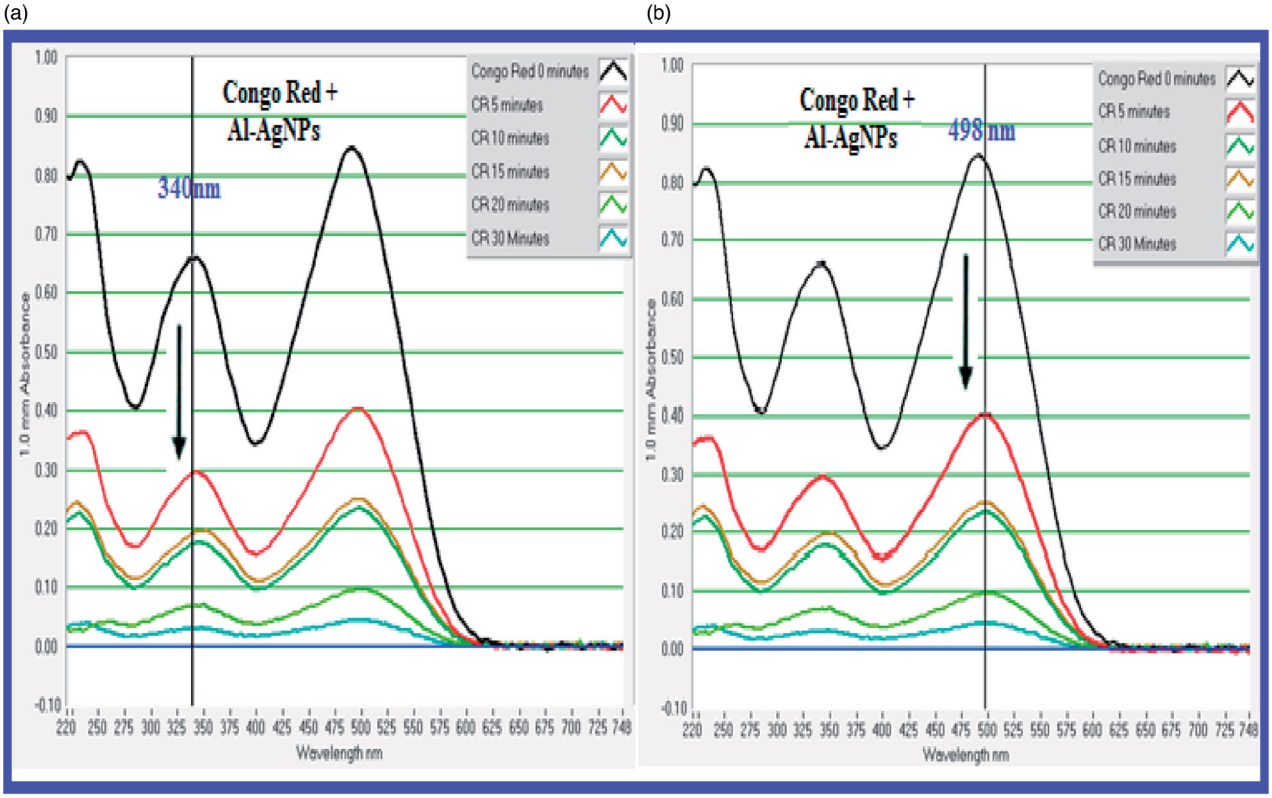

Figure 7. (a) UV-Vis spectra of Congo red dye degradation at different time intervals. (b) Congo red dye degradation—UV-Vis spectra absorbance at different time intervals.

Table 4. UV-Vis spectra of Congo red dye degradation at different time intervals by silver nanoparticles from *A. lanata* flower extracts.

S. no.	Time interval (min)	340 nm	498 nm
1	0	0.657	0.835
2	5	0.294	0.403
3	10	0.174	0.234
4	15	0.192	0.250
5	20	0.068	0.095
6	30	0.030	0.043

of the CR dye was completed within a time interval of 30 min from bright red color to light red color (Figure 7; Table 4). The degradation of CR dye was due to the SPR effect of the biosynthesized Al-AgNPs. The excited surface electron interacts with the dissolved oxygen molecules thereby producing hydroxyl radicals, while allowing Ag^{+} ions to interact with the anionic CR dye (Wu et al. 2010). Therefore, it was evident that the biosynthesized Al-AgNPs from the plant flower extracts of *A. lanata* showed high potentiality as photocatalytic agent for the CB and CR dye degradation in the presence of sunlight.

3.10.2. Catalytic reduction of 4-nitrophenol to 4-aminophenol

As the reduction of toxic 4-NP to nontoxic 4-AP was performed to know the catalytic activity efficacy of the biosynthesized Al-AgNPs. On addition of $NaBH_4$ to 4-NP, from Figure 8, it could be seen that on addition of $NaBH_4$ the original peak of 4-NP centered at ~317 nm shifts to 400 nm with appearance of bright yellow color (Figure 8(a)). This indicates the formation of sodium phenolate (Wunder et al. 2010) without any change in the absorption maxima with respect to different time intervals. After the addition of 0.3 ml of biosynthesized Al-AgNPs to the above solution, the reduction of 4-NP became rapid which was observed by the decoloration of bright yellow color and the appearance of the absorbance maxima at 278 nm (Figure 8(b)), which was a characteristic of the formation of 4-AP (Pradhan, Pal, and Pal 2002; Premkumar, Lee, and Geckeler 2011). Therefore, the results showed that the biosynthesized Al-AgNPs possessed good catalytic activity potentiality for several biomedical applications.

4. Conclusion

In the present work, *A. lanata* flower extract was used for the green production of AgNPs. The biosynthesized Al-AgNPs were spherically shaped, crystalline with an average particle size of 7 ± 3 nm and high negative Zeta potential. The FTIR analysis showed the presence of several active biocompounds acting as stabilizing and capping agents in the formation of Al-AgNPs. The Al-AgNPs displayed antibacterial activity against both Gram-positive and Gram-negative bacterial strains. The Al-AgNPs presented very good antioxidant activity by the DPPH method compared to H_2O_2 and NO methods. The biosynthesized nanoparticles demonstrated very good photo-catalytic activity which was confirmed by cotton blue and congo red dye decorization/degradation activity by reduction of 4-Nitrophenol to 4-Aminophenol activity. Therefore, we conclude that the

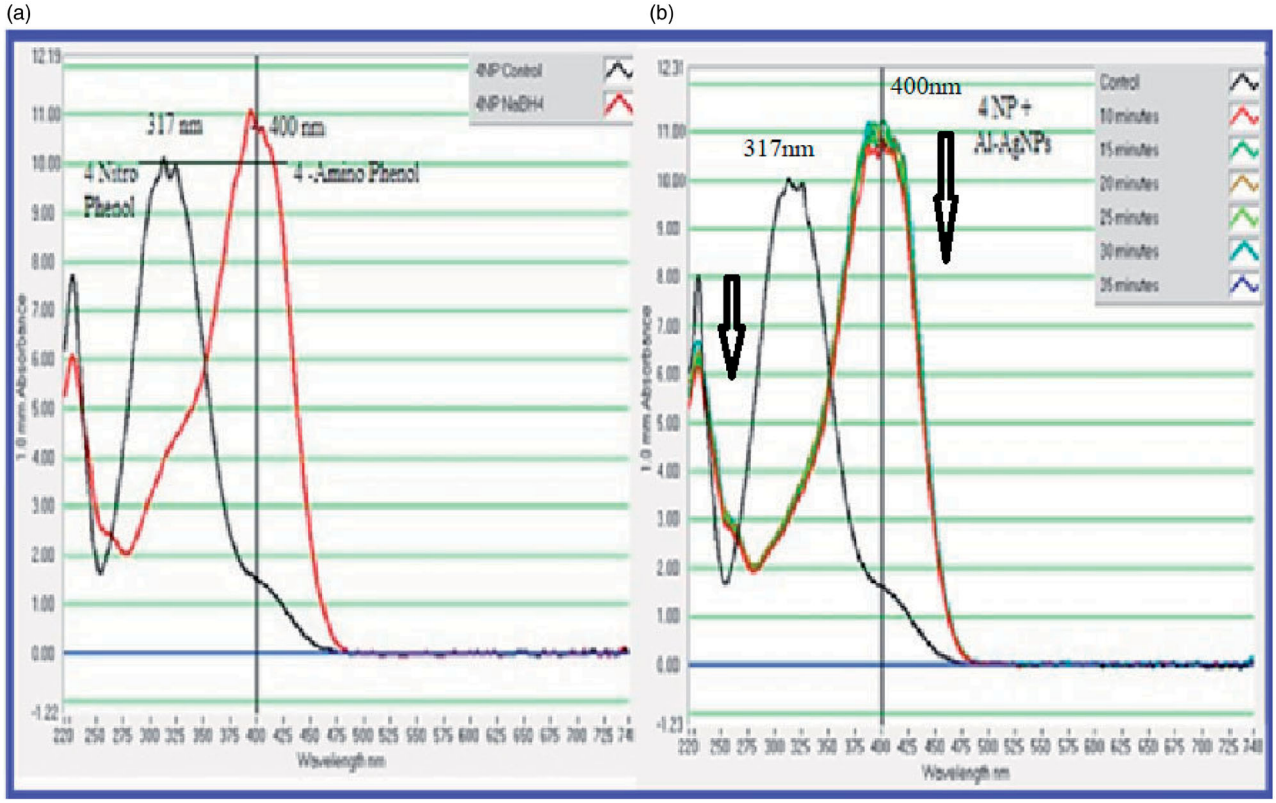

Figure 8. Catalytic activity—UV-Vis spectra: 4-Nitrophenol (4-NP) to 4-Aminophenol (4-AP) reduction, (a) 4-NP + $NaBH_4$, (b) 4-NP + Al-AgNPs at different time intervals.

biosynthesized Al-AgNPs have good biomedical and bio-remediation applications.

Acknowledgments

The authors are grateful to DST PURSE Centre, Sri Venkateswara University, Tirupati, for providing the facility to carry out research activity.

Disclosure statement

No potential conflict of interest was reported by the author(s).

ORCID

Sashikiran Palithya http://orcid.org/0000-0001-9603-5109
Susmila Aparna Gaddam http://orcid.org/0000-0001-7671-3136
Venkata Subbaiah Kotakadi http://orcid.org/0000-0001-7315-3575
Josthna Penchalaneni http://orcid.org/0000-0003-3825-6020
Narasimha Golla http://orcid.org/0000-0002-1760-3321
Suresh Babu Naidu Krishna http://orcid.org/0000-0003-3155-8878
C. V. Naidu http://orcid.org/0000-0002-3610-7200

References

Abdulmutalib, U. S., and M. Manjur. 2017. Phytochemical screening on the antioxidant properties of *Aerva lanata* flower extracts and their in vitro anti-proliferative effects on human liver cancer cell line (HEPG-2) running head-phytochemical screening of flower extracts of *Aerva lanata*. *Journal of Biology and Nature* 7 (2):81–90.

Afsheen, S., H. Naseer, T. Iqbal, M. Abrar, A. Bashir, and M. Ijaz. 2020. Synthesis and characterization of metal sulphide nanoparticles to investigate the effect of nanoparticles on germination of soybean and wheat seeds. *Materials Chemistry and Physics* 252:123216. doi: 10.1016/j.matchemphys.2020.123216.

Ajitha, B., Y. A. K. Reddy, and P. S. Reddy. 2015. Biosynthesis of silver nanoparticles using *Momordica charantia* leaf broth: Evaluation of their innate antimicrobial and catalytic activities. *Journal of Photochemistry and Photobiology B: Biology* 146:1–9. doi:10.1016/j.jphotobiol.2015.02.017.

Al-Shmgani, H. S., W. H. Mohammed, G. M. Sulaiman, and A. H. Saadoon. 2017. Biosynthesis of silver nanoparticles from Catharanthus roseus leaf extract and assessing their antioxidant, antimicrobial, and wound-healing activities. *Artificial Cells, Nanomedicine, and Biotechnology* 45 (6):1234–40. doi:10.1080/21691401.2016.1220950.

Athira, P., and S. N. Nair. 2017. Pharmacognostic review of medicinal plant *Aerva lanata*. *Journal of Pharmaceutical Sciences and Research* 9 (9):1420.

Bauer, A. W., W. M. Kirby, J. C. Sherris, and M. Turck. 1966. Antibiotic susceptibility testing by a standardized single disk method. *American Journal of Clinical Pathology* 45 (4_ts):493–6. doi: 10.1093/ajcp/45.4_ts.493.

Dauthal, P., and M. Mukhopadhyay. 2013. Biosynthesis of palladium nanoparticles using *Delonix regia* leaf extract and its catalytic activity for nitro-aromatics hydrogenation. *Industrial & Engineering Chemistry Research* 52 (51):18131–9. doi:10.1021/ie403410z.

Emam, H. E., M. K. Zahran, and H. B. Ahmed. 2017. Generation of biocompatible nanogold using H_2O_2–starch and their catalytic/antimicrobial activities. *European Polymer Journal* 90:354–67. doi:10.1016/j.eurpolymj.2017.03.034.

Fatimah, I., and Z. H. V. I. Aftrid. 2019. Characteristics and antibacterial activity of green synthesized silver nanoparticles using red spinach (*Amaranthus tricolor* L.) leaf extract. *Green Chemistry Letters and Reviews* 12 (1):25–30. doi:10.1080/17518253.2019.1569729.

Francis, S., S. Joseph, E. P. Koshy, and B. Mathew. 2018. Microwave assisted green synthesis of silver nanoparticles using leaf extract of *Elephantopus scaber* and its environmental and biological

applications. *Artificial Cells, Nanomedicine, and Biotechnology* 46 (4):795–804. doi:10.1080/21691401.2017.1345921.

Gaddam, S. A., V. S. Kotakadi, D. V. R. Sai Gopal, Y. Subba Rao, and A. Varada Reddy. 2014. Efficient and robust biofabrication of silver nanoparticles by *Cassia alata* leaf extract and their antimicrobial activity. *Journal of Nanostructure in Chemistry* 4 (1):82. doi:10.1007/s40097-014-0082-5.

Ghosh, S., P. Sumersing, A. Mehul, K. Rohini, K. Sangeeta, P. Karishma, S. S. Cameotra, J. Bellare, D. D. Dhavale, and A. Jabgunde. 2012. Synthesis of silver nanoparticles using *Dioscorea bulbifera* tuber extract and evaluation of its synergistic potential in combination with antimicrobial agents. *International Journal of Nanomedicine* 7:483.

Golla, N. 2018. Phytosynthesis and antimicrobial studies of silver nano particles using *Ziziphus nummularia* leave extracts. *MOJ Drug Design Development & Therapy* 2 (5):4.

Goyal, M., A. Pareek, B. P. Nagori, and D. Sasmal. 2011. *Aerva lanata*: A review on phytochemistry and pharmacological aspects. *Pharmacognosy Reviews* 5 (10):195. doi:10.4103/0973-7847.91120.

Gupta, S. S., J. Sharma, G. Rajesh Kumar, G. Pandey, P. K. Mohapatra, A. K. S. Rawat, and C. V. Rao. 2014. Effect of *Andrographis serpyllifolia* leaves extract on experimentally induced typhoid using *Salmonella typhi*. *Journal of Pharmaceutical Research International* 4 (2):230–9.

He, W., Y.-T. Zhou, W. G. Wamer, M. D. Boudreau, and J.-J. Yin. 2012. Mechanisms of the pH dependent generation of hydroxyl radicals and oxygen induced by Ag nanoparticles. *Biomaterials* 33 (30): 7547–55. doi:10.1016/j.biomaterials.2012.06.076.

Hussain, I., N. B. Singh, A. Singh, H. Singh, and S. C. Singh. 2016. Green synthesis of nanoparticles and its potential application. *Biotechnology Letters* 38 (4):545–60. doi:10.1007/s10529-015-2026-7.

Ijaz, M., M. Aftab, S. Afsheen, and T. Iqbal. 2020. Novel Au nano-grating for detection of water in various electrolytes. *Applied Nanoscience* 10 (11):4029–36. doi:10.1007/s13204-020-01520-w.

Ijaz, M., M. Zafar, and T. Iqbal. 2020. Green synthesis of silver nanoparticles by using various extracts: A review. *Inorganic and Nano-Metal Chemistry* 51 (5):744–755. doi:10.1080/24701556.2020.1808680.

Iqbal, T., G. Ara, N. R. Khalid, and M. Ijaz. 2020. Simple synthesis of Ag-doped CdS nanostructure material with excellent properties. *Applied Nanoscience* 10 (1):23–8. doi:10.1007/s13204-019-01044-y.

Khan, T. H., and S. Sultana. 2006. Apigenin induces apoptosis in Hep G2 cells: Possible role of TNF-α and IFN-γ. *Toxicology* 217 (2–3): 206–12. doi:10.1016/j.tox.2005.09.019.

Khatami, M., I. Sharifi, M. A. Nobre, N. Zafarnia, and M. R. Aflatoonian. 2018. Waste-grass-mediated green synthesis of silver nanoparticles and evaluation of their anticancer, antifungal and antibacterial activity. *Green Chemistry Letters and Reviews* 11 (2): 125–34. doi:10.1080/17518253.2018.1444797.

Kirubha, R., and G. Alagumuthu. 2015. Investigation of antibacterial properties of silver nanoparticles using *Aerva lanata* extract. *Indo American Journal of Pharmaceutical Sciences* 2 (3):668–75.

Kotakadi, V. S., S. A. Gaddam, S. K. Venkata, P. V. G. K. Sarma, and D. V. R. Sai Gopal. 2016. Biofabrication and spectral characterization of silver nanoparticles and their cytotoxic studies on human CD34+ ve stem cells. *3 Biotech* 6 (2):216. doi:10.1007/s13205-016-0532-5.

Kotakadi, V. S., S. A. Gaddam, S. K. Venkata, and D. V. R. Sai Gopal. 2015. New generation of bactericidal silver nanoparticles against different antibiotic resistant *Escherichia coli* strains. *Applied Nanoscience* 5 (7):847–55. doi:10.1007/s13204-014-0381-7.

Kumar, K. P., W. Paul, and C. P. Sharma. 2011. Green synthesis of gold nanoparticles with *Zingiber officinale* extract: Characterization and blood compatibility. *Process Biochemistry* 46 (10):2007–13. doi:10.1016/j.procbio.2011.07.011.

Litvin, V. A., and B. F. Minaev. 2013. Spectroscopy study of silver nanoparticles fabrication using synthetic humic substances and their antimicrobial activity. *Spectrochimica Acta Part A: Molecular and Biomolecular Spectroscopy* 108:115–22. doi:10.1016/j.saa.2013.01.049.

Maiti, S., S. Purakayastha, and B. Ghosh. 2007. Production of low-cost carbon adsorbents from agricultural wastes and their impact on dye adsorption. *Chemical Engineering Communications* 195 (4):386–403. doi:10.1080/00986440701707917.

Mata, R., J. R. Nakkala, and S. Rani Sadras. 2015. Biogenic silver nanoparticles from *Abutilon indicum*: Their antioxidant, antibacterial and cytotoxic effects in vitro. *Colloids and Surfaces B: Biointerfaces* 128: 276–86. doi:10.1016/j.colsurfb.2015.01.052.

Nagaratna, A., Prakash, L. Hegde, and A. Harini. 2015. A pharmacological review on *Gorakha ganja* (*Aerva lanata* (Linn) Juss. Ex. Schult). *Journal of Pharmacognosy and Phytochemistry* 3 (5):35–9.

Naidu, K. S. B. 2020. Engineered nanoparticles: Hazards and risk assessment upon exposure-A review. *Current Trends in Biotechnology & Pharmacy* 14 (1):111–22.

Netala, V. R., S. Bukke, L. Domdi, S. Soneya, S. G. Reddy, M. Satyanarayana Bethu, V. S. Kotakdi, K. V. Saritha, and V. Tartte. 2018. Biogenesis of silver nanoparticles using leaf extract of *Indigofera hirsuta* L. and their potential biomedical applications (3-in-1 system). *Artificial Cells, Nanomedicine, and Biotechnology* 46 (sup1):1138–48. doi:10.1080/21691401.2018.1446967.

Netala, V. R., V. S. Kotakadi, P. Bobbu, S. A. Gaddam, and V. Tartte. 2016. Endophytic fungal isolate mediated biosynthesis of silver nanoparticles and their free radical scavenging activity and anti microbial studies. *3 Biotech* 6 (2):132. doi:10.1007/s13205-016-0433-7.

Oliveira, L. S., A. S. Franca, T. M. Alves, and S. D. F. Rocha. 2008. Evaluation of untreated coffee husks as potential biosorbents for treatment of dye contaminated waters. *Journal of Hazardous Materials* 155 (3):507–12. doi:10.1016/j.jhazmat.2007.11.093.

Paramasivam, R., D. S. Raj, A. S. Chinthamony, G. Thangarajan, and K. Velliyur. 2012. Phytochemical screening, antioxidant activity of *Aerva lanata* (L)–An in vitro study. *Asian Journal of Pharmaceutical and Clinical Research* 5 (2):77–81.

Payal, C., K. Gurlaganjeet, K. Davinder, S. Gagan, and C. Amit. 2015. A review on phytochemistry and biological activities of *Aerva*. *Medicinal & Aromatic Plants* 4 (2):187. doi:10.4172/2167-0412.1000187.

Pradhan, N., A. Pal, and T. Pal. 2002. Silver nanoparticle catalyzed reduction of aromatic nitro compounds. *Colloids and Surfaces A: Physicochemical and Engineering Aspects* 196 (2–3):247–57. doi:10.1016/S0927-7757(01)01040-8.

Premkumar, T., K. Lee, and K. E. Geckeler. 2011. Shape-tailoring and catalytic function of anisotropic gold nanostructures. *Nanoscale Research Letters* 6 (1):547. doi:10.1186/1556-276X-6-547.

Ramamurthy, C. H., M. Padma, I. D. Mariya Samadanam, R. Mareeswaran, A. Suyavaran, M. S. Kumar, K. Premkumar, and C. Thirunavukkarasu. 2013. The extra cellular synthesis of gold and silver nanoparticles and their free radical scavenging and antibacterial properties. *Colloids and Surfaces B: Biointerfaces* 102:808–15. doi:10.1016/j.colsurfb.2012.09.025.

Rauwel, P., S. Küünal, S. Ferdov, and E. Rauwel. 2015. A review on the green synthesis of silver nanoparticles and their morphologies studied via TEM. *Advances in Materials Science and Engineering* 2015:1–9. doi:10.1155/2015/682749.

Reddy, B. P., K. Mallikarjuna, G. Narasimha, and S.-H. Park. 2017. Plectranthus amboinicus-mediated silver, gold, and silver-gold nanoparticles: Phyto-synthetic, catalytic, and antibacterial studies. *Materials Research Express* 4 (8):085010. doi:10.1088/2053-1591/aa80a2.

Rees, D. D., R. M. Palmer, and S. Moncada. 1989. Role of endothelium-derived nitric oxide in the regulation of blood pressure. *Proceedings of the National Academy of Sciences of the United States of America* 86 (9):3375–8. doi:10.1073/pnas.86.9.3375.

Revathi, S. L., S. Kumar, V. Sudarshana Deepa, and S. Kumar. 2014. Antimicrobial activity of *A. serpyllifolia* (Rohl. Ex. Vahl) Wright. *International Journal of Pharmaceuticals and Health Care Research* 1:2249–57.

Rodríguez-Gattorno, G., D. Díaz, L. Rendón, and G. O. Hernández-Segura. 2002. Metallic nanoparticles from spontaneous reduction of silver(I) in DMSO. Interaction between nitric oxide and silver

nanoparticles. *The Journal of Physical Chemistry B* 106 (10):2482–7. doi:10.1021/jp012670c.

Saiganesh, S., T. Krishnan, G. Narasimha, H. Almoallim, S. Alhari, L. Reddy, K. Mallikarjuna, A. Mohammed, and V. Prabhakar. 2021. Phytosynthetic fabrication of lanthanum ion-doped nickel oxide nanoparticles using *Sesbania grandiflora* leaf extract and their antimicrobial properties. *Crystals* 11 (2):124. doi:10.3390/cryst11020124.

Seku, K., B. R. Gangapuram, B. Pejjai, K. K. Kadimpati, and N. Golla. 2018. Microwave-assisted synthesis of silver nanoparticles and their application in catalytic, antibacterial and antioxidant activities. *Journal of Nanostructure in Chemistry* 8 (2):179–88. doi:10.1007/s40097-018-0264-7.

Silvia, N., C. H. Rajeswari, D. Mounica, R. Manasa, and D. Prasanth. 2014. Pharmacognostic and phytochemical studies on flowers of *Aerva lanata* [L.] Juss. ex. Schult. *Pharmacognosy Journal* 6 (5):29–32. doi:10.5530/pj.2014.5.6.

Suresh, A. K., M. J. Doktycz, W. Wang, J.-W. Moon, B. Gu, H. M. Meyer, I. I. I. D. K. Hensley, D. P. Allison, T. J. Phelps, and D. A. Pelletier. 2011. Monodispersed biocompatible silver sulfide nanoparticles: Facile extracellular biosynthesis using the γ-proteobacterium, *Shewanella oneidensis*. *Acta Biomaterialia* 7 (12):4253–8. doi:10.1016/j.actbio.2011.07.007.

Tamilarasi, P., and P. Meena. 2020. Green synthesis of silver nanoparticles (Ag NPs) using *Gomphrena globosa* (Globe amaranth) leaf extract and their characterization. *Materials Today: Proceedings* 33:2209–16. doi:10.1016/j.matpr.2020.04.025.

Turunc, E., O. Kahraman, and R. Binzet. 2021. Green synthesis of silver nanoparticles using pollen extract: Characterization, their electrochemical and antioxidant activities. *Analytical Biochemistry* 621:114123. doi:10.1016/j.ab.2021.114123.

Vaishnavi, V., K. K. Sadasivuni, D. Ponnamma, and N. Golla. 2020. Green synthesis of silver nanoparticles from *Pterocarpus santalinus* leaf broth and their antibacterial and antioxidant activities. *Macromolecular Symposia* 392 (1):2000079. doi:10.1002/masy.202000079.

Vanaja, M., K. Paulkumar, M. Baburaja, S. Rajeshkumar, G. Gnanajobitha, C. Malarkodi, M. Sivakavinesan, and G. Annadurai. 2014. Degradation of methylene blue using biologically synthesized silver nanoparticles. *Bioinorganic Chemistry and Applications* 2014:1–8. doi:10.1155/2014/742346.

Vidhya, R., and R. Udayakumar. 2015. Antibacterial potential of different parts of *Aerva lanata* (L.) against some selected clinical isolates from urinary tract infections. *British Microbiology Research Journal* 7 (1):35–47. doi:10.9734/BMRJ/2015/15738.

Wu, Z.-C., Y. Zhang, T.-X. Tao, L. Zhang, and H. Fong. 2010. Silver nanoparticles on amidoxime fibers for photo-catalytic degradation of organic dyes in waste water. *Applied Surface Science* 257 (3):1092–7. doi:10.1016/j.apsusc.2010.08.022.

Wunder, S., F. Polzer, Y. Lu, Y. Mei, and M. Ballauff. 2010. Kinetic analysis of catalytic reduction of 4-nitrophenol by metallic nanoparticles immobilized in spherical polyelectrolyte brushes. *The Journal of Physical Chemistry C* 114 (19):8814–20. doi:10.1021/jp101125j.